# A Novel Coordinated Control of Renewable Energy Sources and Energy Storage System in Islanded Microgrid

Gui, Yonghao; Li, Mingshen; Guerrero, Josep M.; Quintero, Juan Carlos Vasquez

*Published in:*
Proceedings of the 2018 Annual American Control Conference (ACC)

*DOI (link to publication from Publisher):*
10.23919/ACC.2018.8430920

*Publication date:*
2018

*Document Version*
Accepted author manuscript, peer reviewed version

# A Novel Coordinated Control of Renewable Energy Sources and Energy Storage System in Islanded Microgrid

Yonghao Gui, *Member, IEEE*, Mingshen Li, *Student Member, IEEE*, Josep M. Guerrero, *Fellow, IEEE*, and Juan C. Vasquez, *Senior Member, IEEE*

***Abstract*— A novel coordinated control for energy storage system (ESS) and renewable energy source (RES) units is proposed in islanded AC microgrids without a phase-locked loop system. We use a proportional-resonant control technique for the ESS, which fixes the voltage and frequency of the microgrid. Moreover, we use a voltage-modulated direct power control (VM-DPC) technique, which has not only a good tracking performance but also a good steady-state behavior, for the RESs that generate their maximum power in the normal operation. To ensure the stability of the microgrid, we use the passivity property for RESs when the VM-DPC is sued. Hence, the whole system is still stable and passive after integrating the heterogeneous RESs into the microgrid. To validate the proposed coordinated control architecture, we use MATLAB/Simulink, SimPowerSystems to simulate a microgrid consisting of one ESS, one wind turbine, one photovoltaic and two controllable loads. Simulation results show that the islanded microgrid is operating well and the plug-and-play capability of the RESs is enhanced.**

## I. Introduction

Nowadays, with the rapid development of renewable generation, the renewable energy sources (RESs) such as photovoltaic (PV) and wind turbine (WT) systems have been the main sources in microgrids. A microgrid should be able to overcome the intermittent nature of RES. Therefore, energy storage systems (ESSs) are required for the care of grid-fault, energy-shortage, and load fluctuations. Hence, the coordinated control is needed to guarantee stored energy balance among ESSs and RESs to enhance microgrid system stability and reliability [1], [2].

This coordinated problem has been addressed by centralized control and decentralized control concerning the communication links. In centralized control, as a crucial element, the communication channels are able to enhance the stability of microgrid [3]–[5]. A coordinated control strategy with the consideration of state of charge (SoC) balancing in AC microgrid was proposed by combing communication technology with hierarchical control structure [6]. However, the control method will cause the invalidation of intact high-level control functions is inevitable. In [7], a centralized coordinated control was employed to equalize the SoC, even for different capacities of distributed ESSs. But the drawback is that, when a single point failure occurs in one of the communication links, the overall system loses its coordination. A multi-master-slave-based control was proposed to provide rapid load sharing with consideration of distant groups, while the coupling of active and reactive powers problem appears in long transformation [8].

Another method, decentralized coordinated control for balancing discharge rate of ESSs, is an effective method to prevent overcurrent and unintentional outage of RES units, and to provide fast response and large stability margin in an islanded microgrid [9]. Wu *et al.* proposed an autonomous active power control strategy to realize decentralized power management, which relies on local controllers without external communication links. In [10], an independent control is implemented in each unit using multi-loop controllers to autonomously supply power only during peak load periods and keep power balance. However, these two control conditions depend on the PV system, while the various RESs are still not considered. A coordinated and integrated control for PV and ESSs was proposed based on $V$-$f$ (or $P$-$Q$) control, maximum power point tracking (MPPT) control, and ESS charging and discharging control [11]. This algorithm still needs independent parameters that are not adaptive to the system conditions [12]. Recently, some distributed control methods were also proposed to enhance the performance of the microgrids. Distributed cooperative control using feedback linearization [13], distributed-averaging proportional–integral controller [14], droop-free distributed method [15], and consensus-based distributed coordination method [16] were proposed to achieve bounded voltage and accurate reactive power sharing in microgrids.

The aforementioned methods have a synchronization process with a phase-locked loop (PLL) when RESs are integrated into the existing microgrids. Moreover, the stability analysis of the microgrids becomes more complex after the heterogeneous RESs are integrated. To overcome these issues, a novel coordinated control architecture is proposed in islanded AC microgrids including RES/ESS units without PLL. We use a conventional proportional-resonant (PR) controller for the ESS, which supports the voltage and frequency of the microgrid, For the RES, we use a voltage modulated direct power control (VM-DPC), which has some advantages as good tracking and steady-state performances [17]. We can expect that the VM-DPC enhances the plug-and-play ability of RESs since they are integrated into the existing microgrids without the synchronization process using the PLL. In order to ensure the stability, we use the passivity principle, which has an advantage that if a group of passive sub-systems is connected through parallel or feedback, the whole system is also passive and stable [18]. That is if each RES connected to the microgrid satisfies passivity, the stability of the microgrid

The authors are with the Department of Energy Technology, Aalborg University, Aalborg 9220, Denmark. (e-mail: yog@et.aau.dk; msh@et.aau.dk; joz@et.aau.dk; juq@et.aau.dk).

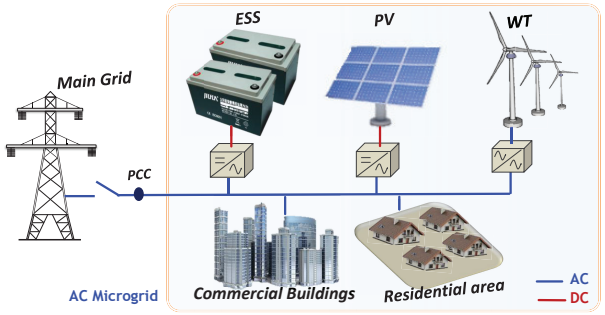


Fig. 1. Architecture of an islanded microgrid

can be guaranteed by using the passivation [19]. Hence, we use the port-controlled Hamiltonian (PCH) for RESs to get the passivity property when the VM-DPC is used. To validate the proposed coordinated control law, we use a microgrid consisting of one ESS, one WT, one PV and two controllable loads. Simulation results show that the islanded microgrid is operating well and the plug-and-play capability of the WT and PV is enhanced.

## II. Review of PR and VM-DPC

In this Section, we briefly introduce PR and VM-DPC controllers.

### A. PR controller of ESS

The PR controller is an effective method to track the voltage/current reference without steady error comparing with PI control. Consequently, the PR controller is used for the ESS to fix the voltage and frequency of the microgrid. The transfer function of the ideal PR controller is

$$G_{PR}(s) = K_P + \frac{K_R s}{s^2 + \omega_0^2}, \tag{1}$$

where $K_P$ and $K_R$ are the controller gains and $\omega_0$ is the angular frequency. Notice that the PR controller has an infinite gain at the frequency $\omega_0$, and there is no phase shift and gain at other frequency [20]. For the simplification, we apply the PR controller to the voltage and current dual loop of ESS in the microgrid. The references of the voltage and frequency of the microgrid are given to the PR controller of the ESS, as shown in Fig. 2.

### B. VM-DPC of RES

For the simplification, this work focuses on the inverter of RES that is directly connected to the microgrid. Fig. 2 shows a RES connected to the microgrid through an inverter with an L-filter. With the consideration of a balanced grid voltage condition, the state-space model of the RES in the $\alpha$-$\beta$ frame is represented as follows:

$$\begin{aligned} v_\alpha &= Ri_{o\alpha} + L\frac{di_\alpha}{dt} + v_{o\alpha}, \\ v_\beta &= Ri_{o\beta} + L\frac{di_\beta}{dt} + v_{o\beta}, \end{aligned} \tag{2}$$

where $v_\alpha$, $v_\beta$, $i_{o\alpha}$, $i_{o\beta}$, $v_{o\alpha}$, and $v_{o\beta}$ represent the converter voltages, line currents, and grid voltages in the $\alpha$-$\beta$ frame, respectively. $R$ and $L$ are the filter resistance and inductance, respectively. We define the output active and reactive powers of the RES in the $\alpha$-$\beta$ frame as follows [21]:

$$\begin{aligned} P &= \frac{3}{2}(v_{o\alpha}i_{o\alpha} + v_{o\beta}i_{o\beta}), \\ Q &= \frac{3}{2}(v_{o\beta}i_{o\alpha} - v_{o\alpha}i_{o\beta}), \end{aligned} \tag{3}$$

where $P$ and $Q$ are the output active and reactive powers of the RES, respectively. Based on a nondistorted grid, the state-space model of the output active and reactive powers could be obtained based on the grid voltage variations.

$$\begin{aligned} \dot{P} &= -\frac{R}{L}P - \omega Q + \frac{3}{2L}(v_{o\alpha}v_\alpha + v_{o\beta}v_\beta - V_g^2), \\ \dot{Q} &= \omega P - \frac{R}{L}Q + \frac{3}{2L}(v_{o\beta}v_\alpha - v_{o\alpha}v_\beta), \end{aligned} \tag{4}$$

where $\omega$ is the angular frequency of the voltage and $V_g = \sqrt{v_{o\alpha}^2 + v_{o\beta}^2}$. VM-DPC control inputs could be defined as [22]

$$u_{vm} = \begin{bmatrix} u_{vmP} \\ u_{vmQ} \end{bmatrix} = \begin{bmatrix} v_{o\alpha}v_\alpha + v_{o\beta}v_\beta \\ -v_{o\beta}v_\alpha + v_{o\alpha}v_\beta \end{bmatrix}. \tag{5}$$

Consequently, the original system (4) is rewritten such as

$$\begin{aligned} \dot{P} &= -\frac{R}{L}P - \omega Q + \frac{3}{2L}(u_{vmP} - V_g^2), \\ \dot{Q} &= \omega P - \frac{R}{L}Q + \frac{3}{2L}u_{vmQ}. \end{aligned} \tag{6}$$

We define errors of active and reactive powers such as

$$e_1 = P^d - P, \quad e_2 = Q^d - Q, \tag{7}$$

where $P^d$ and $Q^d$ denote the references of active and reactive powers, respectively.

**Theorem 1:** [22] Consider the new system in (6), if a control law is taken such as

$$u_{vm} = \begin{bmatrix} u_{vmP} \\ u_{vmQ} \end{bmatrix} = \begin{bmatrix} V_g^2 + \frac{2R}{3}P + \frac{2L\omega}{3}Q + \nu_P \\ \frac{2L\omega}{3}P - \frac{2R}{3}Q - \nu_Q \end{bmatrix}, \tag{8}$$

where $\nu_P = \dot{x}_1^d + K_{P,p}e_1, \nu_Q = \dot{x}_2^d + K_{Q,p}e_2$, $K_{P,p} > 0$ and $K_{Q,p} > 0$, then the closed-loop system is globally exponentially stable. ◊

*Proof:* We differentiate the active and reactive powers until at least one of the VM-DPC control inputs appears.

$$\begin{bmatrix} \dot{P} \\ \dot{Q} \end{bmatrix} = \begin{bmatrix} -\frac{R}{L}P - \omega Q + \frac{3}{2L}(u_{vmP} - V_g^2) \\ \omega P - \frac{R}{L}Q - \frac{3}{2L}u_{vmQ} \end{bmatrix}. \tag{9}$$

If we take the control inputs $u_{vmP}$ and $u_{vmQ}$ as (8), then the outputs have a linear relationship with the new control inputs,

$$\dot{P} = \nu_P, \quad \dot{Q} = \nu_Q. \tag{10}$$

Thus, we can get two simple decoupled tracking dynamics for active and reactive powers as follows;

$$\begin{aligned} \dot{e}_P + K_{P,p}e_P &= 0, \\ \dot{e}_Q + K_{Q,p}e_Q &= 0. \end{aligned} \tag{11}$$

If $K_{P,p} > 0$ and $K_{Q,p} > 0$, then the errors globally exponentially converge to zeros. ■

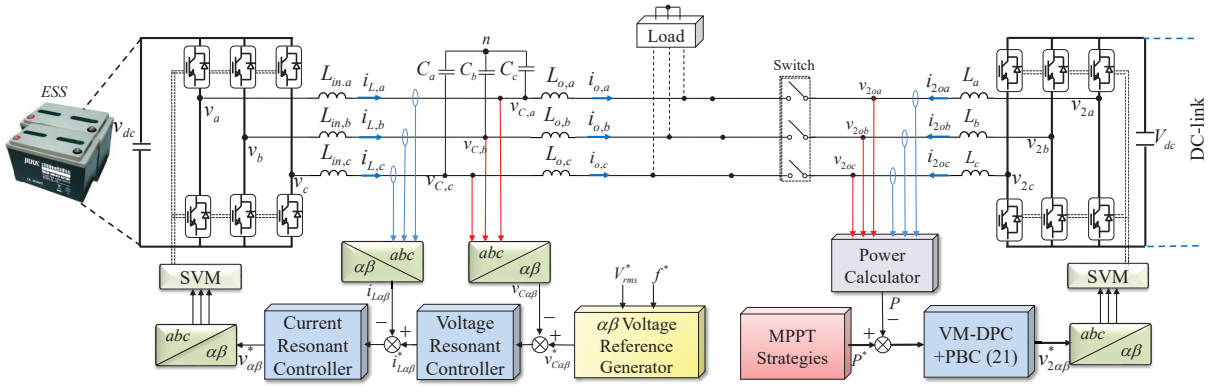


Fig. 2. Block diagram of the proposed coordinated control architecture for RES and ESS.

## III. Passivity-Based Control

In this Section, we discuss the stability of the microgrid when the proposed coordinated control method is used. The stability of DC microgrid has been analyzed in [19], [23]. In this paper, we use passivity property to guarantee the stability of islanded AC microgrid, since the entire system is stable and passive if a set of passive sub-systems is connected through parallel or feedback [18]. Consequently, firstly, we briefly introduce a PCH system, which is used to for RESs to obtain the passivity property when the VM-DPC.

### A. PCH System

Let $x \in \mathbb{R}^n$ denote the state and $u \in \mathbb{R}^m$ denote the input. We consider a system described in the state-space such as

$$\dot{x} = f(x,u), \tag{12}$$

where $x \in \Omega_X \subset \mathbb{R}^n$ indicates the state, and $u \in \Omega_U \subset \mathbb{R}^m$ indicates the input, Moreover, $f(\cdot,\cdot) : X \times U \to \mathbb{R}^n$ is sufficiently smooth in the open connected set $\Omega_X$. Suppose that (12) satisfies a PCH system as

$$\dot{x} = (\mathfrak{J} - \mathfrak{R}) \frac{\partial H(x)}{\partial x} + G(u), \tag{13}$$

where $H$ is a Hamiltonian function given by

$$H(x) = \frac{1}{2} x^T S x, \quad S = S^T \succ 0. \tag{14}$$

Notice that, $S$ is a positive definite matrix. $\mathfrak{R}$ is a positive definite matrix and represents the dissipative forces in the system, $\mathfrak{J}$ is a skew symmetric matrix and represents the conservative forces, and $G(u)$ is the energy acquisition term [24]–[26].

**Assumption 1:** *Suppose that there exist desired input $u^d$ and desired state $x^d$ that satisfy the PCH form* (13)*:*

$$\dot{x^d} = (\mathfrak{J} - \mathfrak{R}) \frac{\partial H(x^d)}{\partial x^d} + G(u^d). \tag{15}$$

$\Diamond$

**Theorem 2:** [27] Suppose a system has the PCH form in (13) with Assumption 1. If $u = u^d$ is applied to the system in (13), then the closed-loop system is exponentially stable. Namely, $\lim_{t\to\infty} x(t) = x^d(t)$. $\Diamond$

We omitted the proof of Theorem 2, which could be found in [27]. $u^d$ could be generated if we use the flatness property. However, in order to use the advantages of the VM-DPC, the controller is modified.

### B. VM-DPC with PCH

In this paper, the new system in (6) satisfies the PCH form (13). If we take a Hamiltonian function as follows:

$$H(x) = \frac{1}{2} x^T S x, \tag{16}$$

where $x = \begin{bmatrix} x_1 & x_2 \end{bmatrix}^T = \begin{bmatrix} P & Q \end{bmatrix}^T$ and $S$ is $2 \times 2$ identity matrix, then the system (6) cab be represented with the PCH form (13) as follows:

$$\dot{x} = (\mathfrak{J} - \mathfrak{R}) \frac{\partial H(x)}{\partial x} + G(u), \tag{17}$$

where

$$\mathfrak{J} = \begin{bmatrix} 0 & \omega \\ -\omega & 0 \end{bmatrix}, \mathfrak{R} = \begin{bmatrix} \frac{R}{L} & 0 \\ 0 & \frac{R}{L} \end{bmatrix}, G(u) = \begin{bmatrix} \frac{3}{2L}(u_{vmP} - V_g^2) \\ \frac{3}{2L} u_{vmQ} \end{bmatrix}.$$

**Assumption 2:** *We define VM-DPC* (8) *as $u^*$, suppose that using $u^*$, $x$ converges to $x^*$. Then, there is a relationship between $x^*$ and $x^d$ in* (15) *such that*

$$x^d - x^* = e^{-\lambda t}(x^d - x), \tag{18}$$

*where $\lambda$ is the decay ratio.* $\Diamond$

Similar assumption is defined for wind turbine system in [28]. From Theorem 1, we can guarantee that the closed loop system is globally exponentially stable with the VM-DPC. Thus, Assumption 2 is acceptable in this study. If we define errors between the desired control input (15) and VM-DPC (8) as follows:

$$\begin{aligned} \Delta u_{vmP} &= u^d_{vmP} - u^*_{vmP} \\ \Delta u_{vmQ} &= u^d_{vmQ} - u^*_{vmQ}, \end{aligned} \tag{19}$$

TABLE I

SYSTEM PARAMETERS USED IN SIMULATION

| Parameter | Symbol | Value |
|---|---|---|
| Nominal bus voltage | $V^*_{rms}$ | 230 V |
| Nominal bus frequency | $f^*$ | 50 Hz |
| Filter inductance of ESS | $L_{in}$ | 1.8 mH |
| Filter capacitor of ESS | $C$ | 27 $\mu$F |
| Output inductance of ESS | $L_o$ | 1.8 mH |
| Filter inductance of PV&WT | $L_{pv,wt}$ | 3.6 mH |
| P-gain of VM-DPC | $K_{P,p}, K_{Q,p}$ | 100 |
| I-gain of VM-DPC | $K_{P,i}, K_{Q,i}$ | 1000 |
| PR controller of voltage | $K_{P,V}, K_{R,V}$ | 1, 100 |
| PR controller of current | $K_{P,I}, K_{R,I}$ | 100, 1000 |

Based on Assumptions 1 and 2, (19) can be represented as follows:

$$\Delta u_{vmP} = \frac{3}{2L}\left(-\lambda_P e^{-\lambda_P t}\dot{e}_P + e^{-\lambda_P t}\frac{R}{L}e_P + e^{-\lambda_P t}\omega e_Q\right),$$
$$\Delta u_{vmQ} = \frac{3}{2L}\left(\lambda_Q e^{-\lambda_Q t}\dot{e}_Q - e^{-\lambda_Q t}\frac{R}{L}e_Q + e^{-\lambda_Q t}\omega e_P\right), \tag{20}$$

where $\lambda_P$ and $\lambda_Q$ are the decay ratio of $e_P$ and $e_Q$, respectively.

**Assumption 3:** *Suppose that $\forall x \in X_o$, there exist $\Delta_P$ and $\Delta_Q$ that satisfy:*

$$\sup_{\forall x \in X_o} \dot{e}_P = \Delta_Q, \quad \sup_{\forall x \in X_o} \dot{e}_Q = \Delta_Q. \tag{21}$$

$\Diamond$

With consideration of the RES rating, the power of RES is bounded. Also, the states are stabilized in the operating range. Moreover, $e$ and $\dot{e}$ are also bounded due to the given reference. Consequently, Assumption 3 is always acceptable.

**Theorem 3:** Given the system (6), suppose that the Assumptions 1 to 3 hold. If we take a control input including VM-DPC (8) and a new feedback such as

$$u_{vm} = u^*_{vm} + u_{fb}, \tag{22}$$

where $u_{fb} = \left[-\kappa_P|e_P|, \kappa_Q|e_Q|\right]^T$, $\kappa_P \geq \lambda_P\Delta_P, \kappa_Q \geq \lambda_Q\Delta_Q$, then the closed-loop system is exponentially stable. $\Diamond$

Due to the page limit, we omitted the proof of Theorem 3 in this paper. Fig. 2 shows the block diagram of the proposed method. In the normal operation, RES will inject its maximum power to the microgrid. Through Theorem 3, the integrated RESs have the passivity property. Thus, the stability of the microgrid can be guaranteed.

## IV. CASE STUDIES

The effectiveness of the proposed coordinated method is verified following Fig. 1 by using MATLAB/Simulink, SimPowerSystems. The parameters of the system and controller gains are listed in Table I. In the simulation, we use a PI controller in the VM-DPC instead of using (8) to handle the offset problem. It will not lose the stability [17], [29]. The case study is summarized as listed in Table II.

TABLE II

SCENARIOS IN SIMULATION

| Parameter | Symbol | Value | Unit |
|---|---|---|---|
| At 0.3s, load 1 is connected | $P_{l1}$ | 5 | kW |
| At 0.51s, WT is connected | $P_{wt}$ | 8 | kW |
| At 0.71s, PV is connected | $P_{pv}$ | 5 | kW |
| At 1s, load 2 is connected | $P_{l2}$ | 10 | kW |

Fig. 3 describes the tracking performance of the powers when the loads, WT, and PV are connected to the microgrid, and Fig. 4 shows the voltages and currents of the loads. At first, the ESS maintains the bus voltage and frequency in the microgrid. At 0.2 s, the switch $S_1$ is on and the load 1 is connected to the microgrid. At this time, only ESS injects the active power to the microgrid. At 0.51 s, the switch $S_2$ is on and the WT suddenly is connected to the microgrid and generates 8 kW. Fig. 5 shows the currents of the ESS and WT, at 0.51 s, the WT generates the power and injects the currents to the microgrid. The WT supports all the power consumed at the load and the surplus power is flowing into the ESS for its charging, as shown in Fig. 3(a) and (c). The voltages and currents of the load 1 have an overshoot and converge to their operating points in one cycle, as shown in Fig. 6.

After 0.2 s, the PV is suddenly connected to the microgrid and generates 5 kW from Fig. 3(d). At this time, the power ripples in the microgrid are slightly increased and the active power of the load 1 has a small overshoot since the voltages and currents are affected by the connection of the PV, as shown in Fig. 4. Finally, at 1 s, the load 2 (10 kW) is connected to the microgrid. At this time, the total power of RES is less than the total power. Thus, the ESS is discharging its power for supporting the loads. From Fig. 7, the voltages and currents converge to their operating fast, but the connection of the load 2 affects the WT and PV which have a undershoot, as shown in Fig. 3. Moreover, the THD of voltages and currents of the load are less than 5% as commonly required for grid operation. Consequently, we can conclude that the proposed coordinated control strategy for the islanded microgrid has a good effect and the RES could plug into the microgrid anytime.

## V. CONCLUSIONS

A novel coordinated control strategy was proposed in islanded AC microgrids including RESs and ESS to handle the synchronization process without PLL and stability issues. We used the conventional PR controller for the ESS using which supports the voltage of the microgrid, and the VM-DPC for the RESs which injects their maximum power to the existing microgrid in the normal operation. Moreover, we used the passivity principle to guarantee the stability of the microgrid. Finally, simulation results show that the islanded AC microgrid is operating well and the plug-and-play capabilities of the RESs are enhanced.

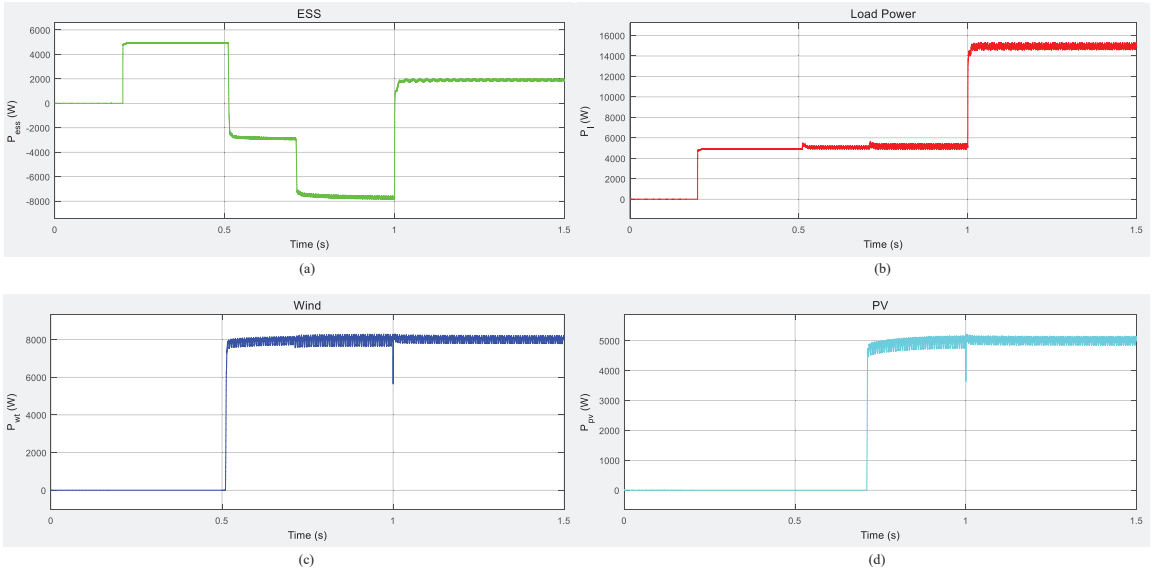


Fig. 3. Active power of (a) ESS, (b) load, (c) WT, and (d) PV, when the proposed coordinated control is used for the islanded microgrid:

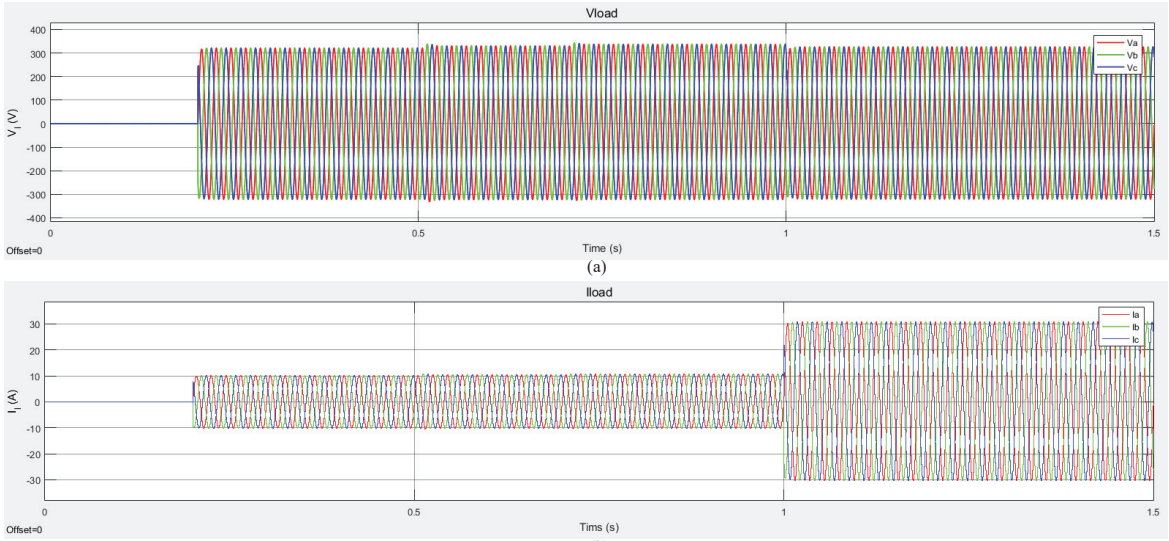


Fig. 4. Voltages and injected currents to the whole loads. (a) Voltages, (b) currents.

## REFERENCES


[1] J. M. Guerrero, J. C. Vasquez, J. Matas, L. G. De Vicuña, and M. Castilla, "Hierarchical control of droop-controlled AC and DC microgrids—A general approach toward standardization," *IEEE Trans. Ind. Electron.*, vol. 58, no. 1, pp. 158–172, 2011.

[2] D. Wu, F. Tang, T. Dragicevic, J. C. Vasquez, and J. M. Guerrero, "A control architecture to coordinate renewable energy sources and energy storage systems in islanded microgrids," *IEEE Trans. Smart Grid*, vol. 6, no. 3, pp. 1156–1166, 2015.

[3] W. Shi, X. Xie, C.-C. Chu, and R. Gadh, "Distributed optimal energy management in microgrids," *IEEE Trans. Smart Grid*, vol. 6, no. 3, pp. 1137–1146, 2015.

[4] J. P. Lopes, C. Moreira, and A. Madureira, "Defining control strategies for microgrids islanded operation," *IEEE Trans. Power Syst,*, vol. 21, no. 2, pp. 916–924, 2006.

[5] X. Lu, K. Sun, J. M. Guerrero, J. C. Vasquez, and L. Huang, "State-of-charge balance using adaptive droop control for distributed energy storage systems in DC microgrid applications," *IEEE Trans. Ind. Electron.*, vol. 61, no. 6, pp. 2804–2815, 2014.

[6] T. Dragičević, J. M. Guerrero, J. C. Vasquez, and D. Škrlec, "Supervisory control of an adaptive-droop regulated DC microgrid with battery management capability," *IEEE Trans. Power Electron.*, vol. 29, no. 2, pp. 695–706, 2014.

[7] N. L. Díaz, A. C. Luna, J. C. Vasquez, and J. M. Guerrero, "Centralized control architecture for coordination of distributed renewable generation and energy storage in islanded AC microgrids," *IEEE Trans. Power Electron.*, vol. 32, no. 7, pp. 5202–5213, 2017.

[8] A. Mortezaei, M. Simoes, M. Savaghebi, J. Guerrero, and A. Al-Durra, "Cooperative control of multi-master-slave islanded microgrid with power quality enhancement based on conservative power theory," *IEEE Trans. Smart Grid*, 2016.

[9] Y. Karimi, H. Oraee, M. S. Golsorkhi, and J. M. Guerrero, "Decentralized method for load sharing and power management in a PV/battery hybrid source islanded microgrid," *IEEE Trans. Power Electron.*, vol. 32, no. 5, pp. 3525–3535, 2017.

[10] H. Mahmood, D. Michaelson, and J. Jiang, "Strategies for independent deployment and autonomous control of PV and battery units in islanded microgrids," *IEEE J. Emerging Sel. Topics in Power Electron.*, vol. 3, no. 3, pp. 742–755, 2015.

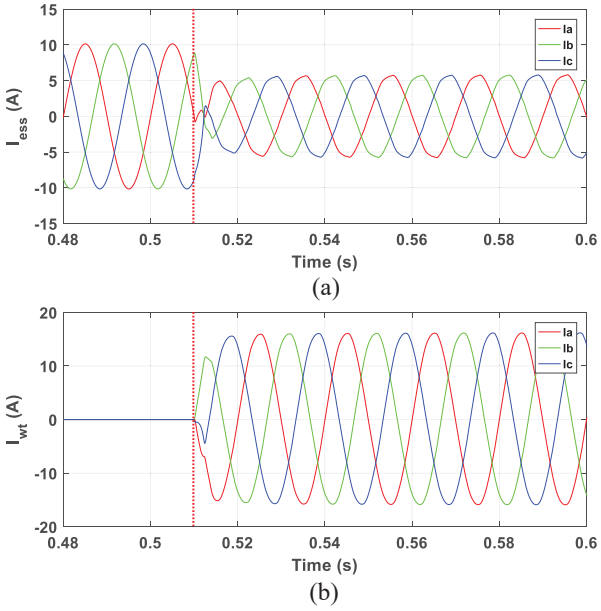


Fig. 5. Currents of (a) ESS and (b) WT, when the WT is connected.

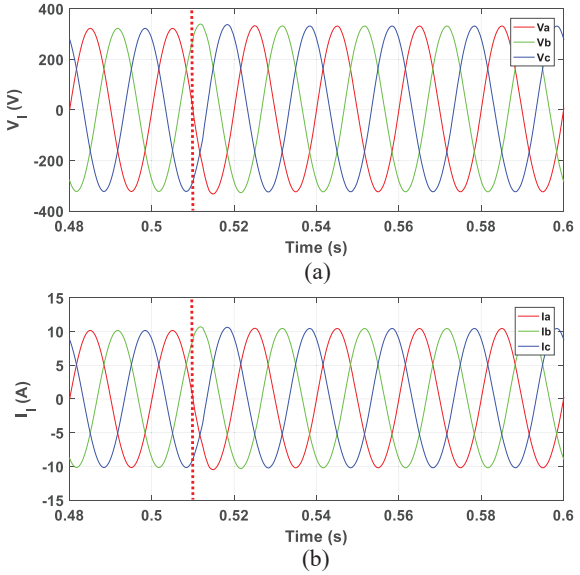


Fig. 6. (a) Voltages and (b) currents of load 1 when the WT is connected.

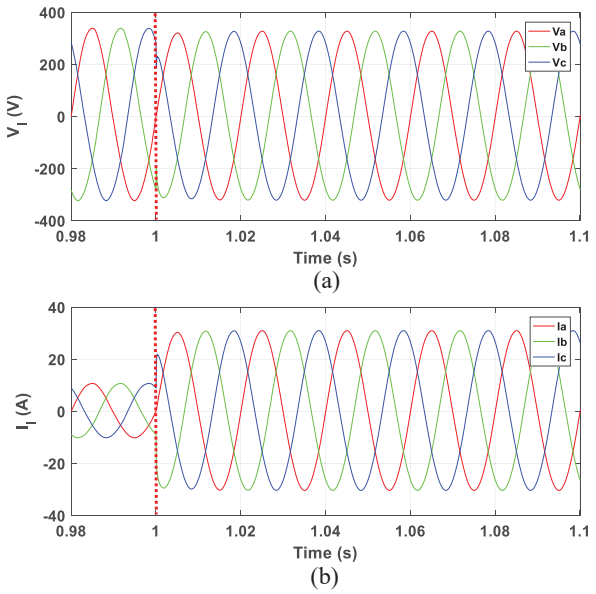


Fig. 7. (a) Voltages and (b) currents of the whole loads when the load 2 is connected.


[11] S. Adhikari and F. Li, "Coordinated Vf and PQ control of solar photovoltaic generators with MPPT and battery storage in microgrids," *IEEE Trans. Smart Grid*, vol. 5, no. 3, pp. 1270–1281, 2014.

[12] H. Mahmood and J. Jiang, "Autonomous coordination of multiple PV/battery hybrid units in islanded microgrids," *IEEE Trans. Smart Grid*, 2017.

[13] A. Bidram, A. Davoudi, F. L. Lewis, and J. M. Guerrero, "Distributed cooperative secondary control of microgrids using feedback linearization," *IEEE Trans. Power Syst.*, vol. 28, no. 3, pp. 3462–3470, 2013.

[14] J. W. Simpson-Porco, Q. Shafiee, F. Dörfler, J. C. Vasquez, J. M. Guerrero, and F. Bullo, "Secondary frequency and voltage control of islanded microgrids via distributed averaging," *IEEE Trans. Ind. Electron.*, vol. 62, no. 11, pp. 7025–7038, 2015.

[15] V. Nasirian, Q. Shafiee, J. M. Guerrero, F. L. Lewis, and A. Davoudi, "Droop-free distributed control for AC microgrids," *IEEE Trans. Power Electron.*, vol. 31, no. 2, pp. 1600–1617, 2016.

[16] R. Han, L. Meng, G. Ferrari-Trecate, E. A. A. Coelho, J. C. Vasquez, and J. M. Guerrero, "Containment and consensus-based distributed coordination control to achieve bounded voltage and precise reactive power sharing in islanded AC microgrids," *IEEE Trans. Ind. Appl.*, vol. 53, no. 6, pp. 5187–5199, 2017.

[17] Y. Gui, C. Kim, C. C. Chung, J. M. Guerrero, Y. Guan, and J. C. Vasquez, "Improved direct power control for grid-connected voltage source converters," *IEEE Trans. Ind. Electron.*, 2018, to be published, doi: 10.1109/TIE.2018.2801835.

[18] H. Khalil, *Nonlinear Systems*, 3$^{rd}$ ed. Prentice Hall, 2002.

[19] Y. Gu, W. Li, and X. He, "Passivity-based control of DC microgrid for self-disciplined stabilization," *IEEE Trans. Power Syst.*, vol. 30, no. 5, pp. 2623–2632, 2015.

[20] R. Teodorescu, F. Blaabjerg, M. Liserre, and P. C. Loh, "Proportional-resonant controllers and filters for grid-connected voltage-source converters," *IEE Proc. Elect. Power Appl.*, vol. 153, no. 5, pp. 750–762, 2006.

[21] F. Z. Peng and J.-S. Lai, "Generalized instantaneous reactive power theory for three-phase power systems," *IEEE Trans. Instrum. Meas.*, vol. 45, no. 1, pp. 293–297, 1996.

[22] Y. Gui, C. Kim, and C. C. Chung, "Grid voltage modulated direct power control for grid connected voltage source inverters," in *Amer. Control Conf.* IEEE, 2017, pp. 2078–2084.

[23] J. Liu, W. Zhang, and G. Rizzoni, "Robust stability analysis of DC microgrids with constant power loads," *IEEE Trans. Power Syst.*, vol. 33, no. 1, pp. 851–860, 2018.

[24] R. Ortega, A. van der Schaft, B. Maschke, and G. Escobar, "Interconnection and damping assignment passivity-based control of port-controlled Hamiltonian systems," *Automatica*, vol. 38, no. 4, pp. 585–596, 2002.

[25] H. Sira-Ramirez and Silva-Ortigoza, *Control design techniques in power electronics devices*. Springer-Verlag London Limited, 2006.

[26] Y. Gui, W. Kim, and C. C. Chung, "Passivity-based control with nonlinear damping for type 2 STATCOM systems," *IEEE Trans. Power Syst.*, vol. 31, no. 4, pp. 2824–2833, 2016.

[27] Y. Gui, D. E. Chang, and C. C. Chung, "Tracking controller design methodology for passive port-controlled Hamiltonians with application to type-2 STATCOM systems," in *Proc. IEEE Conf. Decision Control, Italy*, 2013, pp. 1653–1658.

[28] Y. Gui, C. Kim, and C. C. Chung, "Improved low-voltage ride through capability for PMSG wind turbine based on port-controlled Hamiltonian system," *Int. J. Control Autom. Syst.*, vol. 14, no. 5, pp. 1195–1204, 2016.

[29] Y. Gui, M. Li, J. Lu, S. Golestan, J. M. Guerrero, and J. C. Vasquez, "A voltage modulated DPC approach for three-phase PWM rectifier," *IEEE Trans. Ind. Electron.*, 2018, to be published, doi: 10.1109/TIE.2018.2801841.